

JGR Solid Earth

RESEARCH ARTICLE

10.1029/2023JB026602

Key Points:

- A high-velocity lower continental crust distributes widely in eastern North America
- The seismically fastest and densest lower crust is roughly along the orogenic fronts
- The lower crust densifies through the metamorphic growth of dense minerals

Supporting Information:

Supporting Information may be found in the online version of this article.

Correspondence to:

C. Li,
lic8@sustech.edu.cn

Citation:

Li, C., Hibbard, L., Gao, H., & Williams, M. L. (2023). Seismic evidence for metamorphic densification of the lower continental crust in eastern North America. *Journal of Geophysical Research: Solid Earth*, 128, e2023JB026602. <https://doi.org/10.1029/2023JB026602>

Received 22 FEB 2023

Accepted 15 MAY 2023

Author Contributions:

Conceptualization: Cong Li, Haiying Gao, Michael L. Williams
Data curation: Cong Li, Leon Hibbard
Formal analysis: Cong Li
Funding acquisition: Haiying Gao, Michael L. Williams
Investigation: Cong Li, Leon Hibbard
Methodology: Cong Li
Project Administration: Haiying Gao
Supervision: Cong Li, Haiying Gao, Michael L. Williams
Validation: Cong Li, Leon Hibbard
Visualization: Cong Li, Leon Hibbard
Writing – original draft: Cong Li, Leon Hibbard, Haiying Gao
Writing – review & editing: Cong Li, Haiying Gao, Michael L. Williams

© 2023. American Geophysical Union.
All Rights Reserved.

Seismic Evidence for Metamorphic Densification of the Lower Continental Crust in Eastern North America

Cong Li^{1,2} , Leon Hibbard¹ , Haiying Gao¹ , and Michael L. Williams¹ 

¹Department of Earth, Geographic, and Climate Sciences, University of Massachusetts Amherst, Amherst, MA, USA, ²Now at Department of Earth and Space Sciences, Southern University of Science and Technology, Shenzhen, China

Abstract The composition of the lower continental crust, as well as its formation, growth, and evolution, remains a fundamental subject to be understood. In this study, we carry out a comparative and integrative analysis of seismic tomographic models, teleseismic receiver function results, and Airy isostasy in order to investigate the properties of the lower continental crust in eastern North America. We extract the depths for Vs of 4.0 km/s, 4.2 km/s, and 4.5 km/s from three selected tomographic models and calculate the differences between the Vs depth contours and the Moho depth defined by receiver functions. We then calculate the Airy isostatic Moho depth and its misfit with the receiver-function-defined Moho. Our analysis reveals three key features: (a) the deepening of the Vs depth contours and the strong negative Airy misfit within the U.S. Grenville Province; (b) a seismically faster-than-average and compositionally denser-than-average lowermost crust in the eastern North American Craton and the Grenville Province; and (c) the thickest, seismically fastest, and densest lowermost crust beneath the southern Grenville Front, the southern Grenville-Appalachian boundary, and the U.S.-Canada national border. We suggest that the lower crust of the craton and the Grenville Province has densified through garnet-forming metamorphic reactions during and after orogenesis, contributing to the widely distributed fast-velocity layer. The lower crust beneath the tectonic boundaries could have experienced more extensive garnet growth during orogenesis and emplacement of mafic magma. This study provides new constraints on the seismic and compositional properties of the lower crust in eastern North America.

Plain Language Summary The continental crust provides important clues about the formation and evolution of the Earth. However, the dominant composition of the lower part of the continental crust remains enigmatic, especially in the regions where the seismic velocities are significantly faster than the global average. In this paper, we investigate the properties of the lower continental crust in eastern North America by comparatively analyzing two types of data sets: (a) the variations of seismic velocity within the crust and (b) the variations of the crustal thickness. Our comparative and quantitative analysis reveals that the lower crust of the eastern North American Craton and the Grenville Province is seismically faster and compositionally denser than the global average. The thickest, seismically fastest, and compositionally densest lower crust is roughly along the orogenic fronts and the U.S.-Canada national border. We suggest that garnet growth within the lower crust is a viable mechanism for forming the widely distributed fast-velocity layer in eastern North America. The lower crust may have been further densified through extensive garnet growth and emplacement of mafic magma at a regional scale.

1. Introduction

The continental crust is the outermost layer of the Earth, with the thickness ranging from ~20 km to as much as 80 km depending on the tectonic setting and history. The geochemical composition of the crust holds the key to understanding its formation and modification through geologic time. It has been widely hypothesized that the continental crust was originally formed from magmatic processes at subduction zones, given the similarities in the bulk geochemical compositions between the continental crust and volcanic arc magmas (e.g., Hacker et al., 2015). It is commonly agreed that the upper part of the crust is dominantly felsic in composition, as inferred from outcrops and sediments (e.g., Hacker et al., 2015). However, discrepancies exist about the composition of the lower crust due to the inaccessibility of deep rocks. Several xenolith analyses and heat flow modeling studies suggest that felsic rocks are dominant at least in some lower crust (e.g., Hacker et al., 2015; Williams et al., 2014), while other studies favor a more mafic lower crust (e.g., Huang et al., 2013; Rudnick & Gao, 2013). Seismic properties, such as the wave speed and its gradient with depth, provide critical constraints on the compo-

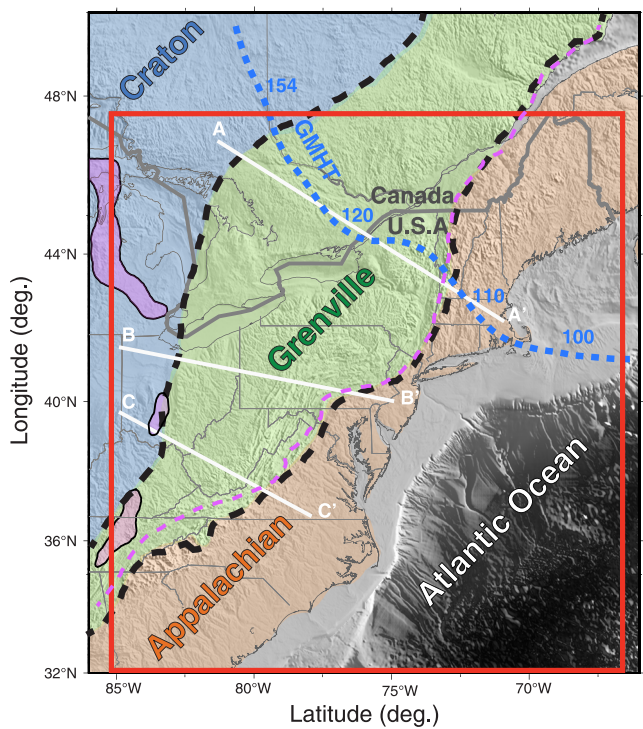


Figure 1. Geological map showing the major tectonic units in eastern North America, modified after Hibbard et al. (2006) and McLelland et al. (2010). The two dashed black lines mark the inferred North American Craton-Grenville boundary (the Grenville Front) and the Grenville-Appalachian boundary. The dashed pink line represents the Appalachian deformation front. The pink patches show the spatial distribution of the Midcontinent Rift based on Stein et al. (2018). The blue dashed line represents the proposed Great Meteor hotspot track (GMHT), marked with time in Ma. The solid gray line marks the U.S.-Canada national border. The three white lines mark the profile locations in Figure 2. The red box shows the imaging area of Figures 3–8.

sition of the continental crust. The crust can be divided into multiple layers in terms of seismic velocities (e.g., Christensen & Mooney, 1995; Hacker et al., 2015): The upper crust has P- and S-wave velocities of $\sim 5.7\text{--}6.4$ km/s and $\sim 3.0\text{--}3.5$ km/s, respectively, and an average thickness of $\sim 12\text{--}14$ km; the middle crust has Vp of $\sim 6.4\text{--}6.8$ km/s and Vs of $\sim 3.5\text{--}3.8$ km/s, and an average thickness of $\sim 7\text{--}13$ km; and the lower crust has Vp of $\sim 6.8\text{--}7.0$ km/s and Vs of $\sim 3.8\text{--}4.0$ km/s, and a thickness varying in a range of $\sim 4\text{--}20$ km. The average Vp and Vs of the uppermost mantle are ~ 8.0 km/s and ~ 4.5 km/s, respectively (Kennett et al., 1995).

Many seismic studies have imaged a relatively fast-velocity layer ($Vp \geq 7.0$ km/s and $Vs \geq 4.0$ km/s) in the lower continental crust at various tectonic regions. Some examples include the central and eastern United States (Schulte-Pelkum et al., 2017), the Rocky Mountains (Gorman et al., 2002), and eastern and northern Australia (Saygin & Kennett, 2012). However, the dominant composition of this fast-velocity layer and its mechanism of formation remain debatable. Some workers have suggested that the composition of the lower crust is dominantly mafic, which has a higher seismic velocity and density than felsic materials (e.g., Huang et al., 2013; Rudnick & Gao, 2013). A variety of tectonic processes have been proposed to explain the enrichment of mafic materials in the lower crust, such as magmatic differentiation at island arcs (Jagoutz & Kelemen, 2015; Kay & Kay, 1991), magma emplacement at rift zones and large igneous provinces (Funck et al., 2000; Marzen et al., 2020; Ridley & Richards, 2010), and attachment of oceanic crust at ancient orogenic belts (Cook, 2002; Dilek & Furnes, 2014). Other workers suggest that garnet can grow within granulites in the lower continental crust through metamorphic reactions, which would increase its density and seismic velocity (e.g., Fischer, 2002; Huang et al., 2019; Jull & Kelemen, 2001; Williams et al., 2014; Xia et al., 2012). In order to provide tighter constraints on the seismic and compositional properties of the lower continental crust, as well as its formation and evolution, an integrative analysis of seismic and geologic datasets is needed.

Eastern North America preserves a complete record of continental assembly and break-up, providing an ideal laboratory for characterizing the seismic properties of the lower continental crust. In this study, we investigate depth

contours of shear-wave velocities that represent the lower crust, the Moho, and the uppermost mantle in eastern North America, based on three seismic tomographic models. We then calculate the depth difference between the velocity contours and the Moho depth defined by teleseismic P-wave receiver function (RF) analysis. We also estimate the isostatic Moho depth in eastern North America using the Airy isostasy hypothesis and compare it with the RF-defined Moho depth. Our study reveals a fast-velocity layer broadly distributed within the lower crust of eastern North America and strong regional/local-scale anomalies along the orogenic fronts and the U.S.-Canada national border. Our result suggests that the lower crust of eastern North America has been significantly modified and densified through geologic time at both continental and regional-scales.

2. Tectonic Setting

2.1. Major Tectonic Units in Eastern North America

Our study region is composed of three major tectonic units (Figure 1): the easternmost North American Craton (Laurentia; $\sim 3.8\text{--}1.3$ Ga), the Grenville Province ($\sim 1.3\text{--}0.98$ Ga), and the Appalachian Orogen ($\sim 0.49\text{--}0.28$ Ga). The amalgamation of the Archean continental blocks at $\sim 2.0\text{--}1.8$ Ga formed the core of the North American Craton (Whitmeyer & Karlstrom, 2007). A sequence of tectonic provinces were accreted onto the North American core between ~ 1.76 and 1.35 Ga (Whitmeyer & Karlstrom, 2007).

The formation and evolution of the Grenville Province is largely inferred based on its northern portion, where the Grenville-aged crust is well exposed on the surface (Rivers, 1997). It has been suggested that the

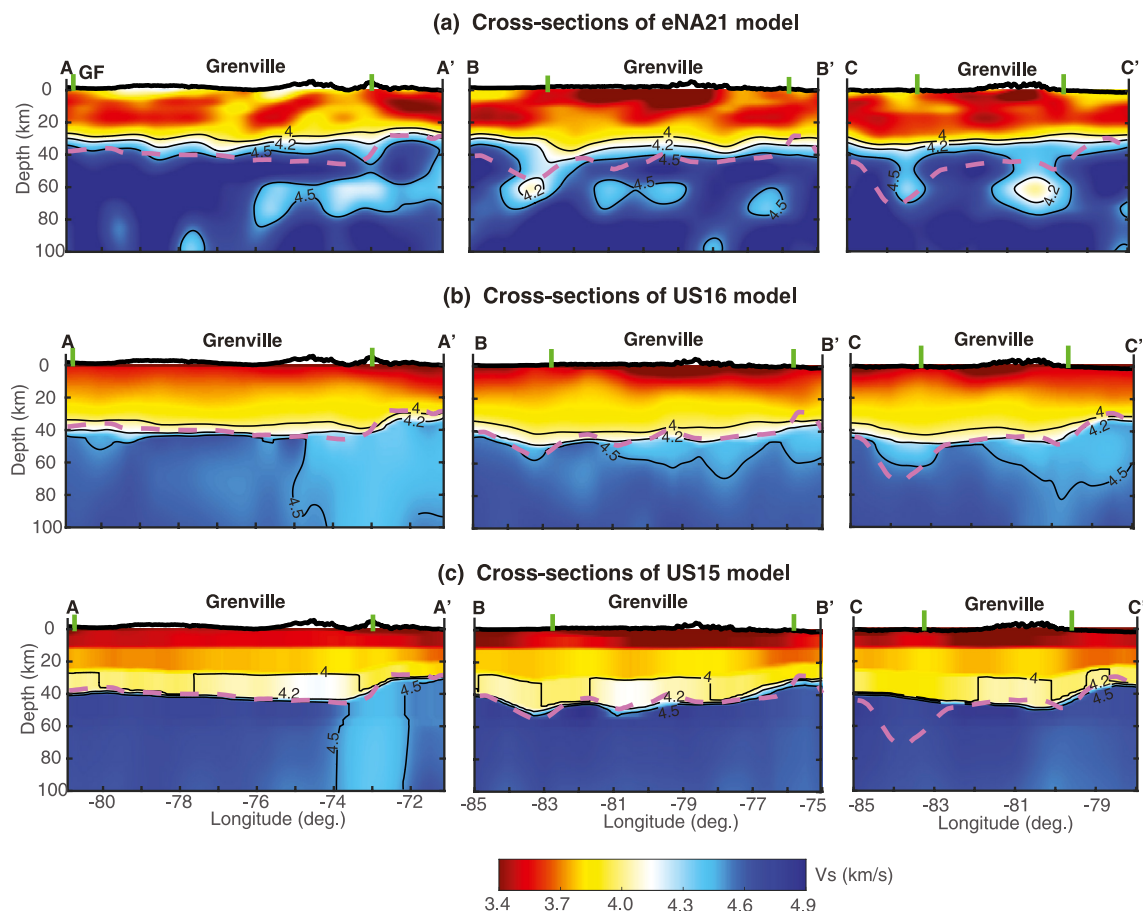


Figure 2. Cross-sections of the shear-wave velocity models of (a) eNA21 by Gao and Li (2021), (b) US16 by Shen and Ritzwoller (2016), and (c) US15 by Schmandt et al. (2015). See the profile locations in Figure 1. The thin black lines mark the depth contours for the shear-wave velocities of 4.0 km/s, 4.2 km/s, and 4.5 km/s, respectively. The pink dashed line denotes the continental Moho after sediment correction, modified after Li et al. (2020). The thick black line on the top of each profile corresponds to the topography, and the vertical green lines mark the North American Craton-Grenville boundary and the Grenville-Appalachian boundary.

Grenville Province was formed through the accretion of a sequence of island arcs and microcontinents onto the eastern margin of the North American Craton during ~ 1.25 – 1.14 Ga (McLennan et al., 2010, 2013). The subsequent collision of Amazonia and North America completed the assembly of the Rodinia supercontinent at ~ 1.05 Ga (McLennan et al., 2010, 2013). The Grenville Province experienced different degrees of extensional collapse and erosion after its formation (Jamieson et al., 2010; McLennan et al., 2010, 2013). Multiple rifting events initiated along the eastern margin of the Grenville Province by ~ 0.75 Ga and ultimately led to the breakup of Rodinia (Hatcher, 2010).

The Appalachian Orogen was formed during the assembly of the Pangea supercontinent from approximately 0.49–0.28 Ga, which involved a sequence of terrane accretions and the ultimate collision of Laurentia with Gondwana (Hatcher, 2010). The main Laurentia-Gondwana collision was concentrated in the central and southern Appalachians and is not considered to have had a major effect on the northern portion (Hatcher, 2010).

Mesozoic rifting occurred from ~ 0.23 Ga to ~ 0.18 Ga and led to the breakup of Pangea and the formation of the modern Atlantic margin (Hatcher, 2010; Withjack et al., 2012). During rifting, the Central Atlantic Magmatic Province (CAMP) was emplaced at ~ 0.2 Ga over a short period. Massive basaltic dikes and sills associated with the CAMP magmas are exposed along the Atlantic margin, although the magmas are more voluminous in the south (Withjack et al., 2012). Fast-velocity anomalies have been imaged within and/or below the lower crust of sedimentary basins along the margin, which are interpreted as magmatic intrusion and/or underplating associated with the CAMP event (Gao et al., 2020; Marzen et al., 2020). After the establishment of the passive margin, North America passed over the Great Meteor hotspot at ~ 0.18 – 0.11 Ga (Figure 1; Heaman & Kjarsgaard, 2000).

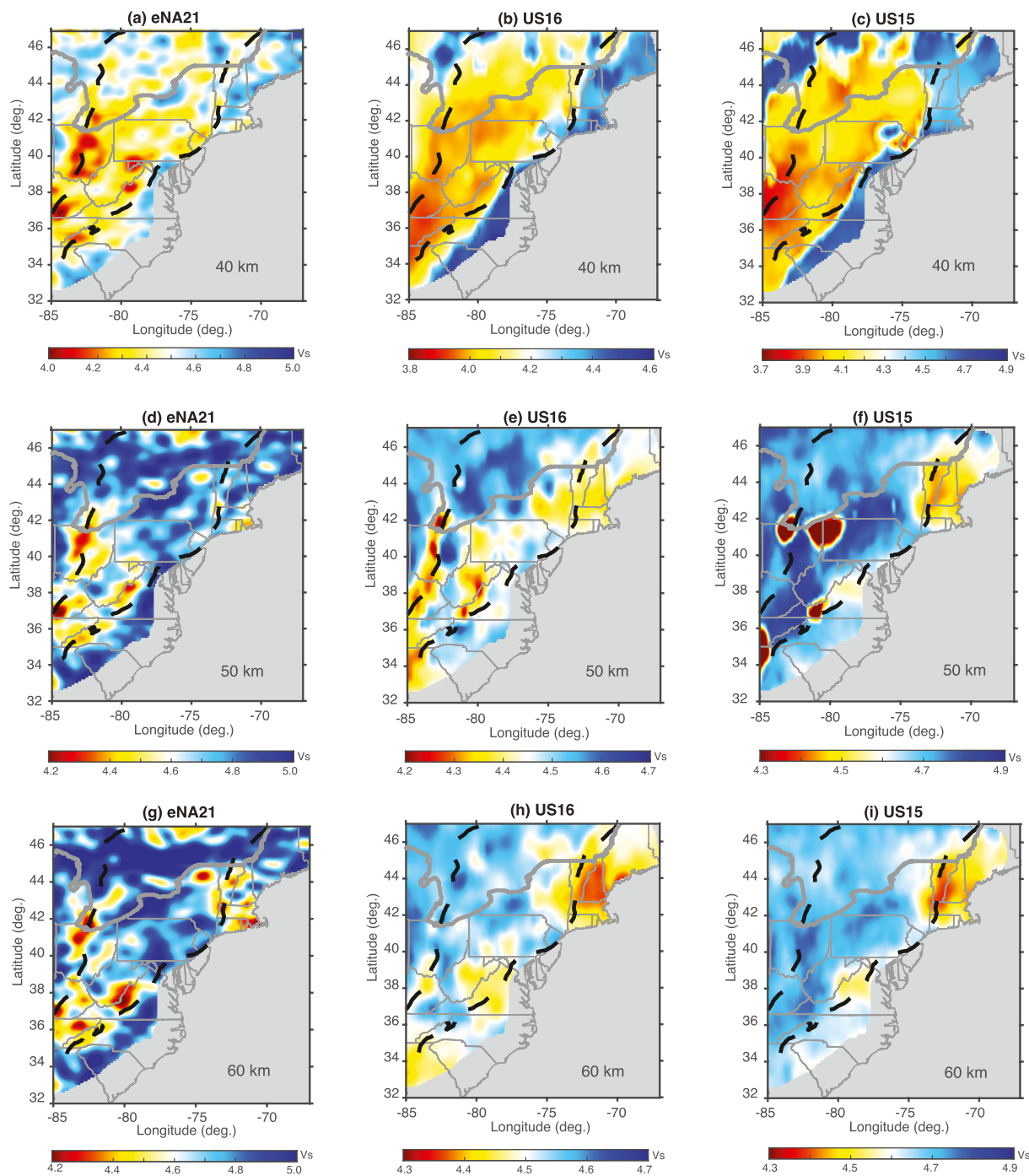


Figure 3. Comparison of the shear-wave velocity models of eNA21 by Gao and Li (2021), US16 by Shen and Ritzwoller (2016), and US15 by Schmandt et al. (2015) at the depths of 40 km (a–c), 50 km (d–f), and 60 km (g–i). The two dashed black lines mark the inferred North American Craton-Grenville boundary and the Grenville-Appalachian boundary. The solid gray line marks the U.S.-Canada national border.

2.2. Major Tectonic Boundaries in Eastern North America

Two major tectonic boundaries, the Grenville Front and the Grenville-Appalachian boundary, are recognized in eastern North America (Figure 1). The Grenville Front is defined as the surface boundary between the eastern North American Craton to the west and the Grenville Province to the east. The northern Grenville Front is well exposed at the surface and has been interpreted as a contractional fault system (McLellan et al., 2010). The Grenville Front was traditionally proposed to extend southward into Ohio and Kentucky in the United States (e.g.,

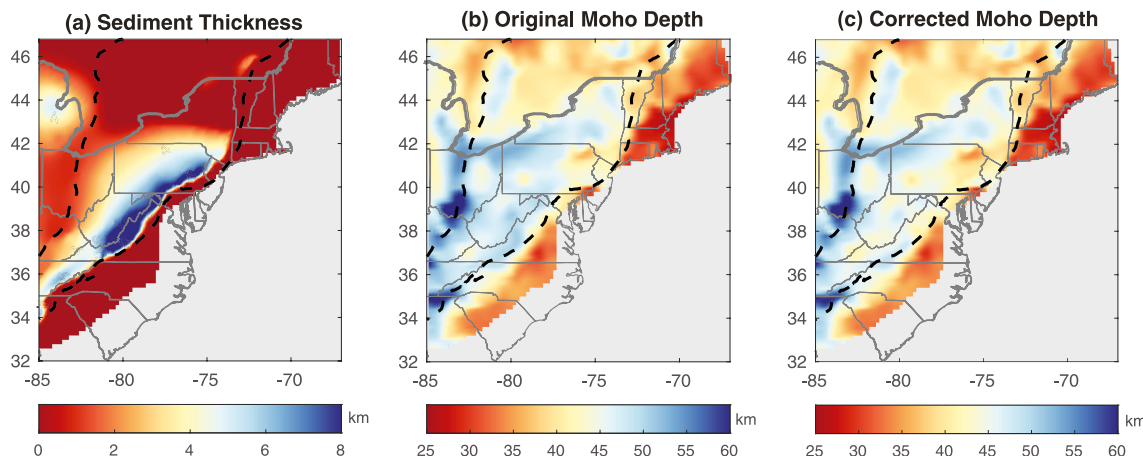


Figure 4. (a) Sediment thickness (in km) within our study region from Mooney and Kaban (2010). (b) Moho depth (in km) defined by teleseismic P-wave receiver functions from Li et al. (2020). (c) Moho depth (in km) after sediment correction, which is used in this study.

Dickas et al., 1992; Stein et al., 2014). Some recent studies, however, suggest that the Midcontinent Rift, a failed rift formed at ~ 1.1 Ga, likely overprinted the southern Grenville Front (Figure 1; e.g., Hinze & Chandler, 2020; Stein et al., 2018).

The Grenville-Appalachian tectonic boundary separates the Grenville-aged rocks to the west and Paleozoic rocks to the east. Its northern portion extends from Eastern Newfoundland, Canada southward to southern New England, and represents the Appalachian deformation front (Figure 1; e.g., Mount, 2014). The Grenville-Appalachian tectonic boundary in the central and southern portions is interpreted to be shallowly dipping under the east of the Appalachian deformation front (Figure 1; e.g., Cook & Vasudevan, 2006; Hynes & Rivers, 2010). In this study, we refer to the Grenville-Appalachian tectonic boundary as our goal is to study the rock properties within the (lower) crust of eastern North America.

3. Material and Methods

In this study, we explore the seismic properties of the lower crust in eastern North America through an integrative analysis of seismic velocity models and teleseismic RF results. First, we select three tomographic models for the crust and mantle lithosphere in eastern North America and compare their similarities and differences. Second, we extract the depths for shear-wave velocities of 4.0 km/s, 4.2 km/s, and 4.5 km/s from each model. We then compare the depth contours for each Vs value with the RF-defined Moho depth. Lastly, we calculate the Airy isostatic Moho depth and its difference from the RF-defined Moho.

3.1. Shear-Wave Velocity Models and Crustal Thickness in Eastern North America

Many seismic tomographic models exist for the crust and mantle lithosphere in eastern North America (e.g., Biryol et al., 2016; Boyce et al., 2019; Chai et al., 2022; and many others), largely benefiting from the deployment of the EarthScope US Transportable Array. In this study, we select three Vs models provided by Gao and Li (2021), Shen and Ritzwoller (2016), and Schmandt et al. (2015). The three models differ in terms of the coverage area, the applied seismic method, the number of seismic stations used, and the model resolution (Figures 2 and 3). Please refer to Table S1 in Supporting Information S1 for a detailed description and comparison of the three models. Hereinafter, we refer to the three models as eNA21 (eastern North America), US16 and US15 (the entire contiguous United States), respectively, in terms of the model coverage area and year of publication.

The variation of the crustal thickness in eastern North America has been the subject of many studies (e.g., Li et al., 2020; Ma & Lowry, 2017; Petrescu et al., 2016; and many others). In this study, we refer to the Moho depth map defined by the P-wave RF analysis of Li et al. (2020) (Figure 4b). Within our study region, the sediment thickness is ~ 5 –13 km in West Virginia and eastern Pennsylvania and up to 5 km in northeastern Michigan (Figure 4a; Mooney & Kaban, 2010). We evaluate and correct the impact of sedimentary layers on the RF-defined

Table 1*A Summary of the Definition of the Parameters Used in This Study*

Parameter	Definition	Physical significance
$D_{Vs=4.X}$	Extracted depth of the shear-wave velocity of 4.X km/s from seismic tomographic models	<ul style="list-style-type: none"> $D_{Vs=4.0}$: the depth of the average Vs of the lowermost crust $D_{Vs=4.2}$: the depth of the Vs that represents the crust–mantle transition zone $D_{Vs=4.5}$: the depth of the average Vs of the uppermost mantle
D_{RF}	Moho depth defined by teleseismic receiver functions from Li et al. (2020), after sediment correction in this study	The depth of the crust–mantle boundary (Moho) defined by receiver functions
$\delta D_{Vs=4.X}$	Depth difference between the extracted depth of Vs = 4.X km/s and the RF-defined Moho, $\delta D_{Vs=4.X} = D_{Vs=4.X} - D_{RF}$	<ul style="list-style-type: none"> A negative value indicates that the Vs = 4.X km/s depth is shallower than the receiver function defined Moho. A positive value indicates that the Vs = 4.X km/s depth is deeper than the receiver function defined Moho.
D_m	Isostatic Moho depth calculated using the Airy model	The depth of the crust–mantle boundary for Airy isostatic equilibrium
δD_{Airy}	Depth difference between the isostatic Moho and the RF-defined Moho, $\delta D_{Airy} = D_m - D_{RF}$	<ul style="list-style-type: none"> A large negative value indicates a mass excess in the crust and/or mantle lithosphere. A large positive value indicates a mass deficit in the crust and/or mantle lithosphere.

Moho depth using the ray-based forward modeling method (Frederiksen & Bostock, 2000). Please see the Supporting Information for a detailed description about the sediment correction. Our analysis demonstrates that ignoring the presence of sediment in the RFs analysis leads to an increase of the estimated Moho depth. On average, every 1-km-thick sedimentary layer results in an error of ~ 1.03 km in Moho depth (Figure S1 in Supporting Information S1). We thus correct the Moho depth data at each grid point provided by Li et al. (2020), based on the thickness of the sediment within our study region (Mooney & Kaban, 2010). We name the RF-defined Moho depth after sediment correction as D_{RF} (Figure 4c).

3.2. Vs Depth Contours in Eastern North America

We extract the depths for shear-wave velocities of 4.0 km/s, 4.2 km/s, and 4.5 km/s, respectively, from US15, US16, and eNA21. The Vs = 4.0 km/s value represents the upper limit of a global-average Vs of the lower continental crust (e.g., Christensen & Mooney, 1995; Hacker et al., 2015; Schulte-Pelkum et al., 2017). The Vs = 4.2 km/s value has been commonly assumed as a proxy for the transition from the lowermost crust to the uppermost mantle (Christensen & Mooney, 1995). And the Vs = 4.5 km/s value represents the global-average Vs of the uppermost mantle immediately beneath the continental Moho (Kennett et al., 1995). Please refer to Table 1 for a summarized description of the parameters defined in this study.

We first interpolate the models vertically from the surface down to 100 km depth at an interval of 1 km. We then search the corresponding depths for each Vs ± 0.03 km/s within a depth range of 15–100 km at every horizontal grid point of the original models. If we find more than one depth value for the given Vs, we accept the shallowest depth in order to avoid the impact of low-velocity anomalies that might exist in the upper mantle. We then interpolate the extracted depths using a uniform grid size of $0.2^\circ \times 0.2^\circ$ to produce the depth contours for each Vs, that is, $D_{Vs=4.0}$, $D_{Vs=4.2}$, and $D_{Vs=4.5}$ (Figure 5 and Figure S5 in Supporting Information S1).

We calculate the depth difference between the Vs depth contours and the RF-defined Moho depth, $\delta D_{Vs} = D_{Vs} - D_{RF}$. The distribution pattern of the δD_{Vs} values (Figure 6) has important implications for the physical properties of the lower crust and the uppermost mantle. Specifically, a large negative $\delta D_{Vs=4.0}$ value likely indicates the presence of a higher-than-average velocity layer at the bottom of the lower crust. Hereinafter, we refer to the layer between $D_{Vs=4.0}$ and D_{RF} , where $\delta D_{Vs=4.0}$ is dominantly negative, as the fast-velocity layer. We calculate the average Vs of the fast-velocity layer and convert it to Vp by assuming a constant Vp/Vs ratio of 1.8. We then estimate the corresponding density using an empirical Vp-density relationship established based on

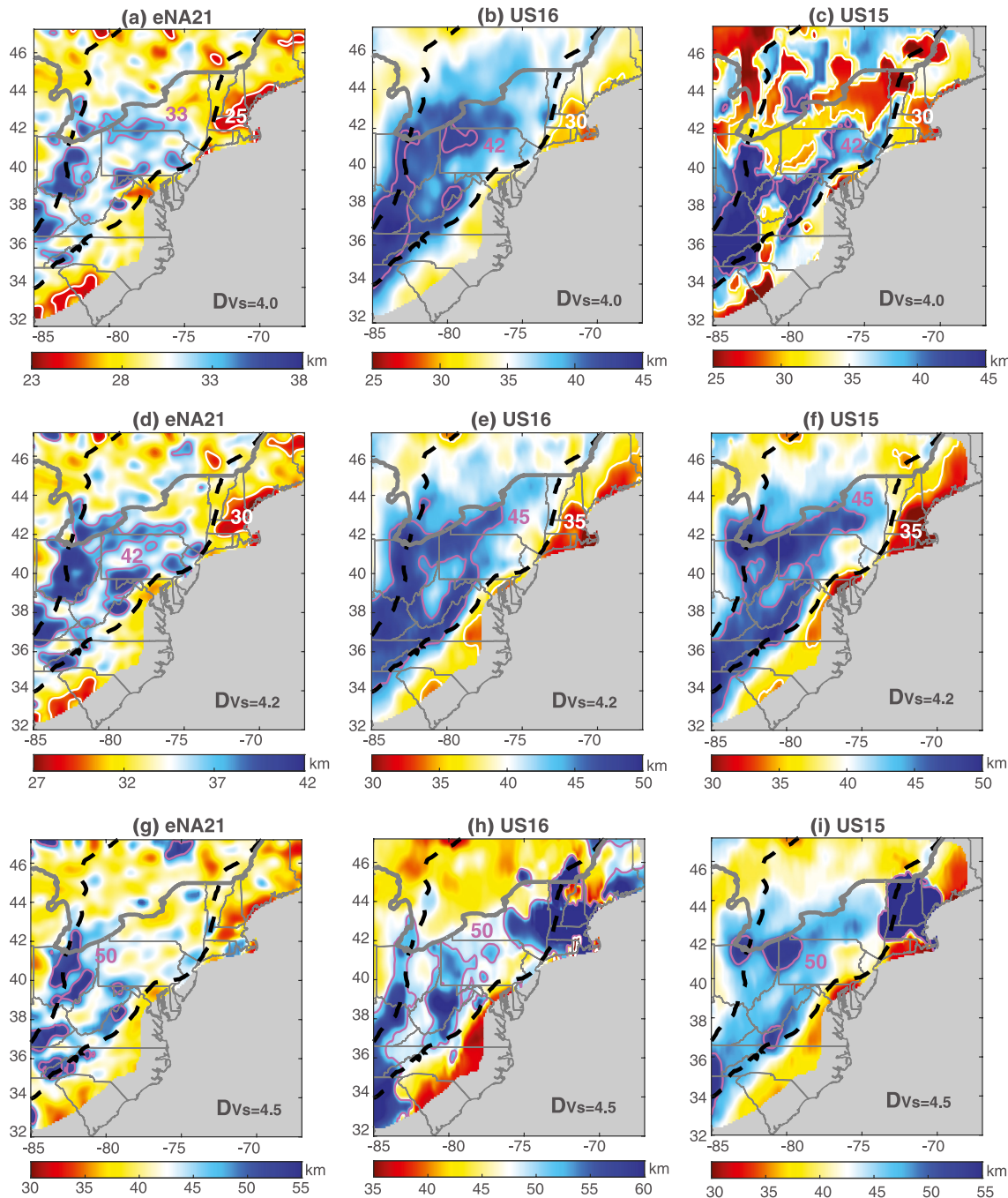


Figure 5. The extracted depth contours (in km) for shear wave velocities of (a–c) $V_s = 4.0 \text{ km/s}$, (d–f) $V_s = 4.2 \text{ km/s}$, and (g–i) $V_s = 4.5 \text{ km/s}$, based on the tomographic models of eNA21 by Gao and Li (2021), US16 by Shen and Ritzwoller (2016), and US15 by Schmandt et al. (2015). Note that for the same V_s depth contour, we choose slightly different color scales for the three models to highlight the similarities of the distribution patterns. The purple and white contours mark the anomalously large and small depths (annotated in each subplot), respectively.

the laboratory measurements of mafic rocks by Barton (1986). The $\delta D_{V_s=4.2}$ map provides a comparison between the crust-mantle transitional depth inferred from the $V_s = 4.2 \text{ km/s}$ depth contour and the RF-defined Moho. And a large positive $\delta D_{V_s=4.5}$ value indicates that the uppermost mantle is seismically slower than the global average of the uppermost mantle. Note that the values and distribution pattern of $D_{V_s=4.5}$ and $\delta D_{V_s=4.5}$ in southern New England differ among the three tomographic models (Figures 5 and 6; Figure S5 in Supporting Information S1), which largely reflects the difference in model resolution for the southern New England low-velocity anomaly (Figures 2 and 3).

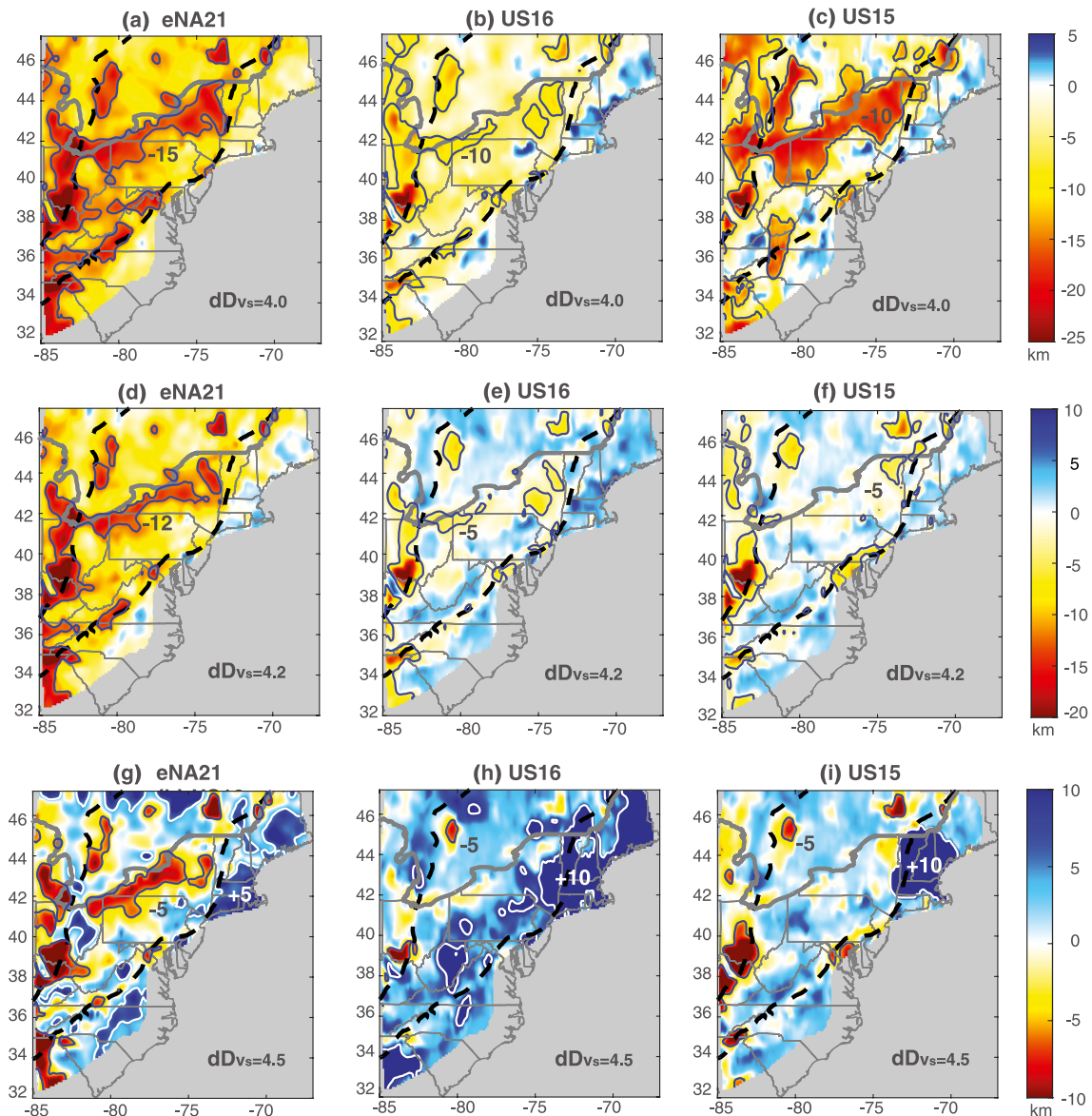


Figure 6. The depth difference (in km) between the Vs depth contours (4.0 km/s, 4.2 km/s, and 4.5 km/s) and the receiver-function defined Moho depth after sediment correction, modified after Li et al. (2020). The negative values in warm color indicate that the Moho depth is greater than the respective Vs depth contour, and vice versa. The black contours in (a)–(i) outline the strong negative values (annotated in each subplot) of the depth differences. The white contours in (g)–(i) outline the strong positive values of the depth differences.

3.3. Airy Isostatic Analysis in Eastern North America

The Airy model hypothesizes that in isostasy, high topographic elevation is compensated by the presence of a deep crustal root and vice versa. In this study, we calculate the Airy isostatic Moho depth, which is defined as

$$D_m = D_{ref} + \left(\frac{\rho_{uc}}{\rho_{um} - \rho_{lc}} \right) E + \left(\frac{\rho_s - \rho_{uc}}{\rho_{um} - \rho_{lc}} \right) S \quad (1)$$

where D_{ref} is the reference Moho depth, and ρ_s , ρ_{uc} , ρ_{lc} , and ρ_{um} are the densities of sediment, upper crust, lower crust, and uppermost mantle in the reference model, respectively (Table S2 in Supporting Information S1). E refers to the elevation from the global relief modelETOPO1 (Amante & Eakins, 2009). We apply a short wavelength filter of 20 km on the elevation data to remove the small-scale effects of the lithospheric flexure on D_m . S refers to the sediment thickness from Mooney and Kaban (2010) (Figure 4a). D_m is the estimated isostatic Moho depth at a $0.2^\circ \times 0.2^\circ$ grid size in our study region (Figure 7a).

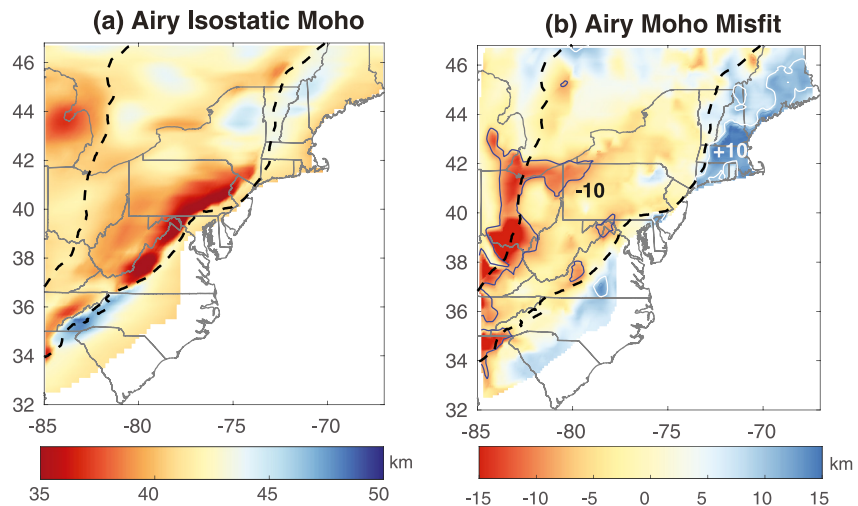


Figure 7. (a) Isostatic Moho depth (in km) calculated based on the Airy model. (b) Depth misfit (in km) between the Airy isostatic Moho depth and the receiver-function defined Moho depth after sediment correction. The negative values in warm colors indicate the observed Moho depth is deeper than the isostatic Moho, and vice versa. The black and white contours represent strong negative (-10 km) and positive ($+10\text{ km}$) depth misfits, respectively.

We define the Airy isostasy misfit, δD_{Airy} , as the depth difference between the Airy isostatic Moho depth and the RF-defined Moho depth, that is, $\delta D_{\text{Airy}} = D_m - D_{\text{RF}}$. A nearly zero value of δD_{Airy} indicates that it is isostatically compensated. A strong positive (or negative) δD_{Airy} value suggests a mass deficit (or excess) within the crust and/or mantle lithosphere. Here we estimate the impact of the density variations within the fast-velocity $\delta D_{V_s=4.0}$ layer in eastern North America on the Airy isostasy misfit. Specifically, we replace the bottom of the reference crust with a fast-velocity layer, using the layer thickness (Figures 6a–6c), velocity (Figures 8a–8c), and density (Figures 8d–8f) at each grid point that we calculated in Section 3.2 (Figures 8g–8i).

3.4. Uncertainties of the Parameters

The uncertainties of our results originate from three primary sources. The first one is the accuracy and resolution of the tomographic models used to extract the depths of the Vs values. The lateral and depth resolutions of tomography depend on the type of seismic data, the number of seismic stations, the model parameterization, and the inversion method used to construct the models (Table S1 in Supporting Information S1). The horizontal resolution of the velocity perturbations near the Moho depth is improved from $\sim 70\text{ km}$ in the US15 and US16 models to $\sim 50\text{ km}$ in eNA21. The velocity gradient across the Moho is likely better constrained in US15 and US16 than in eNA21. Shen and Ritzwoller (2016) statistically estimated the Vs uncertainty in the US16 model, which is less than 1.5% at near Moho depths. However, it is not straightforward to quantitatively estimate the Vs uncertainties of the eNA21 and US15 models, due to the inversion approaches used in Gao and Li (2021) and Schmandt et al. (2015). Nevertheless, the depth contours of each Vs value extracted from the three models reveal many common features (Figure 5). We take the average of the Vs depths extracted at each grid point from the three models and calculate its standard deviation (Figures S2 and S3 in Supporting Information S1). Our analysis demonstrates that the variations of the D_{V_s} values are on average less than 4 km among the three models, with some regional exceptions (Figure S2d–S2f in Supporting Information S1).

The second uncertainty is the Moho depth defined by teleseismic RFs of Li et al. (2020). The accuracy of the RF-defined Moho depth largely depends on the reference velocity model used to convert the RFs from the time domain to the depth domain. Li et al. (2020) demonstrated that a 5% velocity perturbation in the reference model results in a 2-km uncertainty of the Moho depth extracted from the RFs. Li et al. (2020) used the tomographic model of Shen and Ritzwoller (2016) as the reference model, which has the average Vs uncertainty less than 1.5%. Therefore, the Moho depth uncertainty due to the reference velocity model in Li et al. (2020) can be negligible. The crustal Vp/Vs ratios in the Grenville Province and the eastern margin of the North American craton vary within a range of 1.74–1.82 (Ma & Lowry, 2017). Li et al. (2020) assumed a constant Vp/Vs ratio of 1.78 in the RF study, which can lead to $\sim 1\text{ km}$ uncertainty of the Moho depth. Another common difficulty in the RF

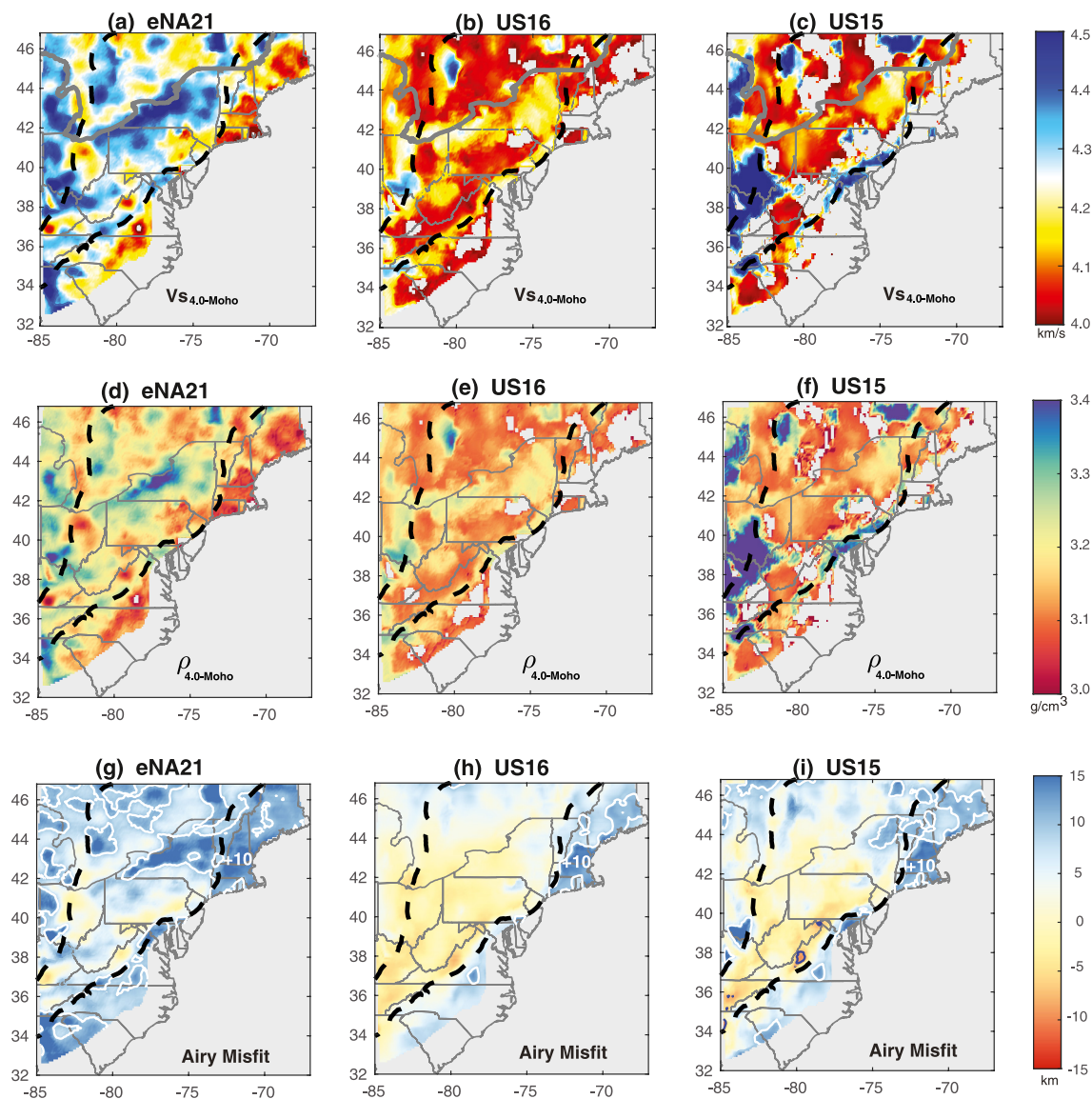


Figure 8. (a–c) Average shear-wave velocities (in km/s) of the layer between the depth contour of $V_s = 4.0$ km/s and the receiver function-defined Moho, based on the models of eNA21 by Gao and Li (2021), US16 by Shen and Ritzwoller (2016), and US15 by Schmandt et al. (2015). (d–f) Average density (in g/cm^3) of the layer between $D_{V_s=4.0}$ and D_{RF} converted from the average velocity in (a–c) using an empirical equation by Barton (1986). (g–i) The corrected Airy Moho misfit (in km) after considering the impact of density perturbations of the layer between $D_{V_s=4.0}$ and D_{RF} . The blue and white contours with annotations in (g–i) represent strong negative and positive anomalies of Airy misfits, respectively.

analysis is choosing the signal that represents the Moho, which is defined as the maximum amplitude of the RFs at 20–70 km depths by Li et al. (2020). Li et al. (2020) examined the regions with extremely thin or thick crust. For example, the seismic stations near the Grenville Front unanimously support the presence of a deep Moho signal (Figure S4 in Supporting Information S1).

The third uncertainty of our results comes from the inherent sensitivities of different types of seismic waves on the depths of sharp velocity discontinuities (e.g., the Moho interface). Surface-wave tomography provides good constraints on the average shear-wave velocities of the crust and upper mantle, and there exists a tradeoff between the Moho depth and seismic velocities near the Moho (e.g., Julia et al., 2000; Shen & Ritzwoller, 2016). In comparison, teleseismic RFs provide important constraints on the depth, sharpness and magnitude of velocity discontinuities (e.g., Rondenay, 2009). Julia et al. (2000) demonstrated that the inversion of surface-wave dispersion curves can lead to a 3–5 km uncertainty on the vertical resolution of V_s depth contours. The vertical resolution of surface-wave tomography can be largely improved by implementing a joint inversion of surface waves

and RFs (e.g., Schmandt et al., 2015; Shen & Ritzwoller, 2016). Gao and Li (2021) constructed the eNA21 model with an advanced wave propagation simulation method and the consideration of the finite frequency sensitivity kernels, which appears to improve the vertical resolution in comparison with the traditional surface-wave imaging methods.

In summary, a variety of factors can contribute to the uncertainties in our analysis. It is unfeasible to provide a quantitative estimate of the uncertainties. In this study, we focus on the common features revealed by the tomographic models and the RF analysis that were independently constructed. This, to a large extent, reflects that our observations to be discussed below do not rely on model selections.

4. Results

The distribution patterns of D_{Vs} , D_{RF} , δD_{Vs} , and δD_{Airy} demonstrate some common features in our study region (Figures 4–7). First, we observe a clear deepening of all the Vs depth contours and the RF-defined Moho depth beneath the U.S. Grenville Province compared to its surroundings. Second, on a large scale, the lower crust of the easternmost North American Craton and the Grenville Province is seismically faster and denser than the global average. And third, the lower crust is the thickest, seismically fastest, and densest along the southern Grenville Front, the southern Grenville-Appalachian boundary, and the U.S.-Canada national border. In the following sections, we describe each of those observations.

4.1. Deepening of Vs Depth Contours and Moho Depth in the U.S. Grenville Province

The deepening of the Vs depth contours within the U.S. Grenville Province is a first-order feature. As inferred from eNA21, the $D_{Vs=4.0}$ value is on average less than 28 km in the easternmost North American Craton, the Canada Grenville Province, and the Appalachian Province (Figure 5a), and $D_{Vs=4.2}$ is on average ~ 33 km beneath those regions (Figure 5d). In comparison, $D_{Vs=4.0}$ and $D_{Vs=4.2}$ fall within the depths of ~ 30 – 38 km (Figure 5a) and ~ 35 – 42 km (Figure 5d), respectively, in the U.S. Grenville Province. The $D_{Vs=4.5}$ contour also shows a deepening beneath the southern U.S. Grenville Province, with local depth maxima of 50–60 km (Figure 5g). The $D_{Vs=4.0}$, $D_{Vs=4.2}$, and $D_{Vs=4.5}$ contours extracted from the US15 and US16 models reveal similar patterns (Figure 5). The depth difference of each Vs value extracted from the three tomographic models primarily reflects the differences in model parameterization and resolution.

The Moho depth map defined by receiver functions reveals a deeper Moho depth beneath the U.S. Grenville Province in comparison with those beneath other regions (Figure 4c). For example, the Moho depth varies within ~ 32 – 45 km beneath easternmost North American Craton and the Canada Grenville Province and within ~ 25 – 45 km beneath the Appalachian Province. In comparison, the Moho depth reaches to ~ 47 – 60 km beneath the U.S. Grenville Province.

4.2. Fast-Velocity Lowermost Crust of Eastern North America

Among the three tomographic models, the distribution patterns of the $\delta D_{Vs=4.0}$, $\delta D_{Vs=4.2}$, and $\delta D_{Vs=4.5}$ maps are largely consistent (Figure 6). For example, the $\delta D_{Vs=4.0}$ values are extensively negative (at a range of -5 km to -20 km) in the craton and the Grenville Province, indicating that the velocity of the lowermost crust is faster than the global average (Figures 6a–6c). The average Vs and densities of this fast-velocity layer vary at a range of ~ 4.2 – 4.4 km/s and ~ 3.0 – 3.2 g/cm³ for the eNA21 model (Figures 8a and 8d), ~ 4.05 – 4.15 km/s and ~ 2.95 – 3.05 g/cm³ for US16 (Figures 8b and 8e), and ~ 4.05 – 4.25 km/s and ~ 2.95 – 3.20 g/cm³ for US15 (Figures 8c and 8f), respectively. The average density variations in the fast-velocity lowermost crust can explain most of the strong negative values of δD_{Airy} (Figures 8g–8i). One exception is the strong positive values of δD_{Airy} in southern New England, which we attribute to the commonly observed low-velocity anomaly in the uppermost mantle (Figures 2 and 3). The Appalachian Province demonstrates the smallest $\delta D_{Vs=4.0}$ (within ± 5 km), indicating that a fast-velocity (lower crust) layer is either very thin or doesn't exist. The widely distributed negative values of $\delta D_{Vs=4.2}$ within the craton suggest that its Moho depth is significantly deeper than the Vs = 4.2 km/s depth contour, further supporting the presence of a fast-velocity lowermost crust. Within the Grenville Province, the $\delta D_{Vs=4.2}$ values are dominantly negative based on eNA21 (at a range of -15 km to -5 km), while showing a mixture of positive and negative values within a narrow range of ± 5 km based on US16 and US15.

Within the interior of the easternmost North American craton and the Grenville Province, the $\delta D_{Vs=4.5}$ map shows weakly positive and negative values (at a range of $-5\text{--}5$ km) based on eNA21, and is dominated by negative values (at a range of -5 to 0 km) based on US16 and US15 (Figures 6g–6i). This indicates that the Vs immediately beneath the RF-defined Moho in the craton and the Grenville Province falls within the global average velocity of the uppermost mantle. In comparison, the $\delta D_{Vs=4.5}$ values based on all the three velocity models show locally positive anomalies (larger than $5\text{--}10$ km) within the Appalachian Province, supporting that the seismic velocity beneath the RF-defined Moho is slower than the global average (Figures 6g–6i).

4.3. Elongated Anomalies Along the Geologic Boundaries and the U.S.-Canada National Border

We observe distinct anomalies of D_{Vs} , D_{RF} , δD_{Vs} , and δD_{Airy} values along the southern Grenville Front, the southern Grenville-Appalachian tectonic boundary, and the U.S.-Canada national border. These observations together support that the lowermost crust beneath the three zones, particularly the central segment of the southern Grenville Front, is thicker, seismically faster, and denser than the surroundings in eastern North America. First, the Vs depth and the RF-defined Moho are exceptionally deep along the three zones (Figures 4c and 5). The $D_{Vs=4.0}$ and $D_{Vs=4.2}$ values along the three zones are greater than 33 and 37 km, respectively, in the eNA21 model, and are greater than 42 and 45 km, respectively, in the US15 and US16 models (Figures 5a–5f). Along the three zones, the $D_{Vs} = 4.5$ values in all three models are >50 km (Figures 5g–5i), and the RF-defined Moho reaches depths of $\sim 52\text{--}60$ km (Figure 4c). Second, the $\delta D_{Vs=4.0}$, $\delta D_{Vs=4.2}$, $\delta D_{Vs=4.5}$, and δD_{Airy} maps reveal some large negative values along the three zones (Figures 6 and 7). For example, in the eNA21 model $\delta D_{Vs=4.0}$ reaches to -15 km, $\delta D_{Vs=4.2}$ reaches -12 km, and $\delta D_{Vs=4.5}$ reaches -5 km along those zones (Figures 6a–6g). Such strong negative values indicate that the RF-defined Moho is significantly deeper than the depths of all extracted velocity contours, that is, a seismically fast lower crust. Likewise, the Airy isostatic misfit is at least -10 km along the three zones (Figure 7b), which suggests a mass excess within the crust. The average Vs and density of the lowermost crust along the three zones are estimated to be approximately 10% faster and 8% higher than the global averages of lower continental crust (Figures 8a–8f). We observe similar deepened features in the US16 and US15 models, though the depth and distribution patterns vary among the models (Figure 6).

5. Discussion

Our analysis, integrating tomographic models, the RF-defined Moho depths, and Airy isostatic models, has revealed that the lowermost crust of the eastern North American craton and the Grenville Province is, in general, seismically faster and compositionally denser than the global averages. Further, the western and eastern margins of the Grenville Province and the boundary between the United States and Canadian portions of the Grenville Province are characterized by particularly fast and dense lower crust. Several previous studies have also suggested the presence of a relatively high-velocity layer in the lower crust in parts of eastern North America, including northern New York (Hughes & Luetgert, 1992; Shalev et al., 1991), the southern Appalachians (Wagner et al., 2012), and the central and eastern United States in general (Schulte-Pelkum et al., 2017; Zhang et al., 2020). Our new findings provide comprehensive maps of thickness, average velocity, and average density of the lowermost crust of eastern North America which, in turn, provide new constraints on its composition and evolution as briefly discussed below.

5.1. Crustal Thickening of the U.S. Grenville Province

The U.S. portion of the Grenville Province has a noticeably thicker crust and deeper Vs depth contours than the Canada portion (Figures 3 and 4). Li et al. (2020) considered two end-member models to explain the difference and both may have played a role. The first is that the Grenville Province was formed through different modes of collision from south to north, which resulted in the difference in crustal thickness that has persisted to the present. The second is that the entire Grenville-aged crust was formed with a nearly uniform thickness, but experienced different degrees of post-orogenic modification. Previous geological and geochemical studies have suggested that the Grenville-aged crust in Canada experienced multiple periods of thinning due to gravitational collapse during and after the Grenville orogeny (e.g., Brudner et al., 2022; Jamieson et al., 2010; McLelland et al., 2013).

Airy isostatic theory predicts thick continental crust in regions of high elevation. However, the average elevation of the U.S. Grenville Province, where the crust is thick (Figure 4), is less than ~ 1 km. This disproportionate

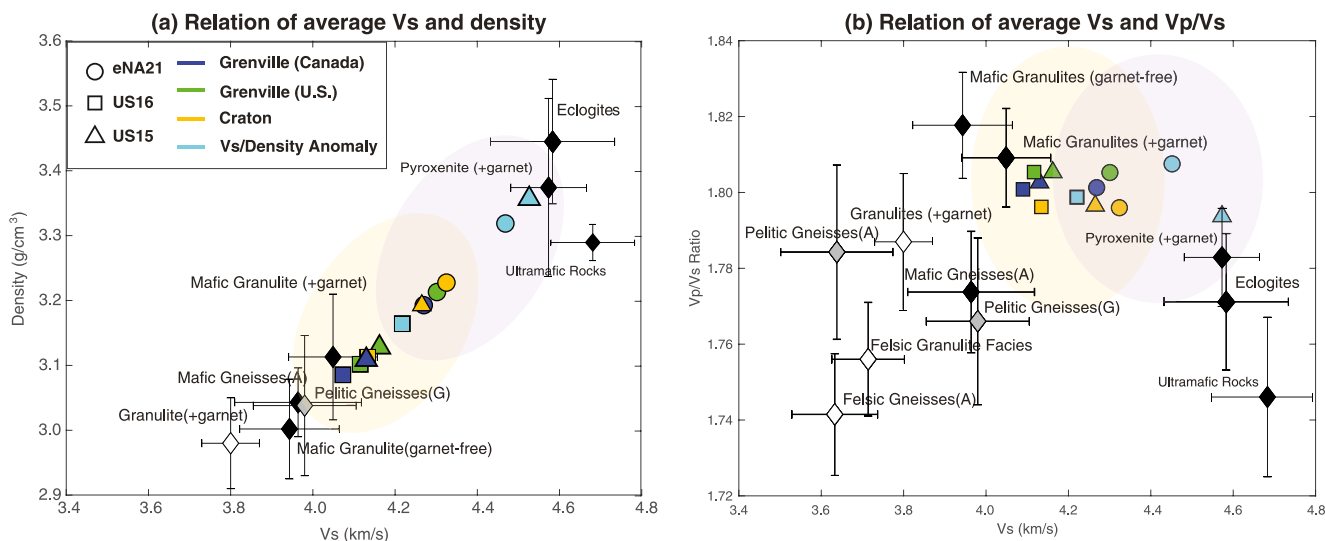


Figure 9. (a) Relationship of the average shear-wave velocity and density of the layer between $D_{\text{Vs}} = 4.0$ and D_{RF} , in comparison with the laboratory measurements of typical lower crustal rocks. The white, gray, and black diamonds mark the shear-wave velocities and density of typical felsic, intermediate, and mafic lower crustal rocks, which are based on the laboratory measurements by Rudnick and Fountain (1995). The blue, green, and orange colors represent the average velocity and density within the Canada Grenville Province, the U.S. Grenville Province, and the easternmost North American Craton, respectively. The cyan colors represent the average values for the regions with large velocities and density anomalies. The orange ellipse marks the distribution range of the averaged velocities and densities within the Grenville Province and the eastern North American craton among the three tomographic models. And the purple ellipse marks the distribution range for the regions where large velocities and density anomalies exist. (b) Relationship of the average shear-wave velocities of the layer between $D_{\text{Vs}} = 4.0$ and D_{RF} and the average crustal Vp/Vs ratio. Other symbols are the same as in the left figure.

relation between elevation and crustal thickness is especially distinct along the margins of the U.S. Grenville Province (Figure 4). We carried out a simple isostatic calculation, based on our analysis of the Grenville Province, to investigate the possible contribution of a dense lower crust. The calculation suggests that a 10-km-thick lowermost crust with a density of 3.2 g/cm^3 could account for an elevation reduction of 1.2 km. This supports the conclusion from seismic data that the density of the Grenville-aged lower crust is much higher than the average of continental crust (Figures 8d–8f). A dense lower crust would tend to resist isostatic rebound during the post-tectonic erosion of the high-altitude paleo-plateau that has been hypothesized to be produced during the Grenville orogeny (Brudner et al., 2022; Jamieson et al., 2010; Rivers, 2008).

Despite the difference in crustal thickness, our analysis suggests that the high-velocity layer beneath the United States and Canadian portions of the Grenville Province is similar in several respects. For example, the thickness of the high-velocity layer is similar in the United States and Canadian portions, although the actual value depends on the tomographic models used in the depth extraction of the shear-wave velocities (Figures 6a–6c). The average Vs of the fast-velocity layer is $\sim 4.12 \text{ km/s}$ within the U.S. Grenville and $\sim 4.08 \text{ km/s}$ within the Canada Grenville, respectively, based on the US16 model (Figures 8b and 9). The corresponding density is $\sim 3.12 \text{ g/cm}^3$ within the U.S. Grenville and $\sim 3.10 \text{ g/cm}^3$ within the Canada Grenville, respectively (Figures 8e and 9). Considering the similarities, we suggest that the high-velocity layers in these two regions formed through similar processes, as discussed below.

5.2. Composition and Formation Mechanism of the Fast-Velocity Lower Crust

The dominant composition and the mechanisms of formation of the fast-velocity layers within the lower continental crust has been the subject of debate and uncertainty (Hacker et al., 2015). We first calculate the average velocity and density of the fast-velocity layer within each tectonic unit using the datasets provided in Figures 8a–8f. We have excluded the Appalachian Province in the calculations because a fast-velocity lowermost crust is either thin or nonexistent beneath this region (Figures 8a–8f). Ma and Lowry (2017) estimated the bulk crustal Vp/Vs ratio of the contiguous United States, which we use to calculate the average Vp/Vs ratio within each tectonic unit of our study region. As shown in Figure 9a, the average Vs and the corresponding density of the lower crust of the eastern North American Craton and Grenville Province are $\sim 4.05\text{--}4.40 \text{ km/s}$ and $\sim 3.08\text{--}3.20 \text{ g/cm}^3$, respectively,

based on the three tomographic models. The average Vp/Vs ratio within the craton and the Grenville Province is about 1.80 (Figure 9b). Our integrative analysis allows us to explore the mechanisms that are responsible for the fast-velocity layer within the continental lower crust.

5.2.1. A Widely-Distributed Fast-Velocity Layer in Eastern North America

It has been suggested that the density of the lower crust can be increased through garnet-forming metamorphic reactions (e.g., Fischer, 2002; Huang et al., 2019; Jull & Kelemen, 2001; Williams et al., 2014; Xia et al., 2012). Several different garnet-forming reactions have been documented in granulite facies rocks during both peak-orogenic metamorphism and post-orogenic cooling. During orogenesis, garnet may form in mafic rocks, especially hydrous mafic rocks, through prograde reactions, such as $\text{Hb} + \text{Pl} = \text{Grt} + \text{Cpx}$, or through partial melting reactions, such as $\text{Hb} + \text{Pl} = \text{Grt} + \text{tonalitic melt}$. In felsic rocks, garnet is commonly produced through biotite dehydration melting reactions, such as $\text{Bt} + \text{Pl} + \text{Als} + \text{Qz} = \text{Grt} + \text{Kfs} + \text{melt}$. In both cases, if melt escapes from the system, the garnet content (and thus density) can be significantly increased, and even rocks with essentially 100% garnet (i.e., garnetites) could have been locally produced (e.g., Dumond et al., 2018).

Significant amounts of garnet can also be produced during retrograde metamorphism, especially at post-orogenic situations that involve nearly isobaric cooling. Retrograde reactions involving the transition from pyroxene-bearing, medium-pressure granulite to high-pressure garnet-bearing granulite can occur during progressive cooling at lower-crustal pressures (ca. 1.0 GPa) (Williams et al., 2014). Thermodynamic modeling suggests that retrograde reactions alone can increase the rock densities to approximately 3.0 g/cm^3 in felsic rocks and significantly above 3.0 g/cm^3 in mafic rocks (Williams et al., 2014). In combination with the products of prograde reactions and partial melting reactions during orogenesis, the densities of the lower crust can likely be higher than 3.0 g/cm^3 . Laboratory measurements have shown that a content of 25–40 vol% garnet within the granulites would increase the density to $\sim 3.15\text{--}3.23 \text{ g/cm}^3$ and the shear-wave velocity to $\sim 4.0\text{--}4.2 \text{ km/s}$ (e.g., Kono et al., 2009; Miller & Christensen, 1994).

The Grenville Province in eastern North America experienced several high-grade tectonometamorphic events. Among those events, the (ca. 1.18–1.14 Ga) Shawinigan orogeny has been interpreted to represent an arc-continent collision, and the (ca. 1.09–1.04 Ga) Ottawan orogeny has been interpreted to involve continent-continent collision. After the Shawinigan orogeny and possibly after the Ottawan orogeny, this region had undergone relatively slow cooling at some depth within the crust before the ultimate exhumation (Brudner et al., 2022; McLelland et al., 2013; Williams et al., 2019). In addition, one or more delamination/founding events have been suggested and would have involved emplacement of mafic magma into the lower crust (McLelland et al., 2013). Considering the long and complex tectonic history, it seems likely that the deep crust of the Grenville Province contains a mix of rock types, including deeply buried metasedimentary rocks, mantle-derived mafic magmatic rocks, and felsic plutonic rocks. The combination of a complex variety of rock types, emplacement of hydrous subduction-related magma and delamination-related mafic magma, multiple high-grade metamorphic events, and slow isobaric cooling, provides an ideal setting for extensive garnet production within the lower crust. We suggest that the high-velocity, high-density lower crust may involve a variety of rock types and processes, but all with a significant content of garnet.

5.2.2. Localized Densification of the Lower Crust

The fastest seismic velocities recognized in this study are located along the southern Grenville Front (i.e., the western edge of the Grenville Province), the southern Grenville-Appalachian boundary and the U.S.-Canada national border. The three regions have the thickest lower crust (Moho depths greater than 50 km) and fastest shear-wave velocities (approaching 4.5 km/s), indicating the presence of very dense rocks ($>3.2 \text{ g/cm}^3$). The correlation of a relatively deep Moho and fast Vs (i.e., dense crustal root) without high topography suggests that these three regions had anomalously thick crust during orogenesis and that the dense roots may have resisted isostatic uplift.

The Vs and inferred density at the lower crust of these three anomalous areas are near the highest end of the range of garnet-bearing crustal rocks (Figure 9). We suggest that the lower crust of these regions may have a larger component of garnet granulite (i.e., garnet, pyroxene, plagioclase, \pm hornblende rocks) than typical heterogeneous lower crust (Kono et al., 2009; Sui et al., 2022). However, garnet-rich restites from partial melting of felsic rocks could also be present (Dumond et al., 2018; Hacker et al., 2015). Further, although plagioclase is expected to be stable at the current pressure/crustal thickness, eclogite (garnet-omphacite) may be locally present in mafic

rocks and has an average density of 3.4–3.5 g/cm³ (Leech, 2001). Previous studies have observed a small component of eclogite in the deep crust beneath the Grenville Front and the southern Grenville-Appalachian boundary (e.g., Indares & Dunning, 1997; Page et al., 2003). It is not surprising that intense tectonism, including crustal thickening and high-P-T metamorphism, may have occurred on the western edge of the Grenville Province during Rodinia assembly and on the eastern edge during Pangea assembly. These two edges are zones of potential strain localization where relatively juvenile rocks were accreted against older, more stable lithosphere. In addition, Williams et al. (2001, 2014) suggested that post-orogenic thermal or deformational events might have promoted cooling-related garnet formation. Midcontinental Rifting may have provided magma and heating in the southern Grenville Front (Stein et al., 2014, 2018) and delamination-related magmatism may have added magma and heating at ca. 50 Ma in the southern Appalachian area (Mazza et al., 2014), both of which could have stimulated additional garnet growth.

It is perhaps more surprising to recognize a region of seismically fast, dense, and thick deep crust near the U.S.-Canadian border within the Grenville Province as this area does not stand out as an obvious tectonic boundary based on surface geology. This may ultimately be one of the unexpected benefits of a study such as ours. It may highlight important tectonic boundaries that are not immediately obvious at the surface and that can benefit from further geologic and geophysical investigation.

6. Conclusions

We conducted an integrative analysis of seismic tomographic models, teleseismic P-wave receiver function results, and Airy isostasy misfit in order to investigate the properties of the lower continental crust in eastern North America. Our analysis recognizes a seismically faster-than-average lowermost crustal layer beneath the easternmost North American Craton and the Grenville Province, with a thickness of ~5–15 km, an average shear-wave velocity of ~4.0–4.4 km/s, and an average density of ~2.95–3.20 g/cm³. The thickest, seismically fastest, and compositionally densest lowermost crust is roughly located along the southern Grenville Front, the southern Grenville-Appalachian boundary, and the U.S.-Canada national border. We suggest that garnet growth during high-P-T metamorphism and partial melting associated with Grenville orogenesis and during post-orogenic isobaric cooling likely contributed to the faster and denser lower crust beneath the Grenville Province. Additional densification, possibly involving extensive garnet growth due to high-grade metamorphism and partial melting during orogenesis and due to emplacement of mafic magma after orogenesis, may be localized in important lithospheric boundaries.

Data Availability Statement

All the data used in this study were obtained from the IRIS Earth Model Collaboration (<https://ds.iris.edu/ds/products/emc-earthmodels/>). The velocity depth contours, the corrected Moho depth, and the average velocity and density of the lowermost crust generated in this study are available on the Open Science Framework website (<https://osf.io/zy5qh/>).

Acknowledgments

This research was supported by the U.S. National Science Foundation under Grant EAR-1930014 awarded to H. Gao and M. L. Williams. We thank the Associate Editor Michael Bostock and two anonymous reviewers for their constructive suggestions.

References

- Amante, C., & Eakins, B. W. (2009). *ETOPO1 arc-minute global relief model: Procedures, data sources and analysis*. National Geophysical Data Center.
- Barton, P. J. (1986). The relationship between seismic velocity and density in the continental crust — A useful constraint? *Geophysical Journal of the Royal Astronomical Society*, 87(1), 195–208. <https://doi.org/10.1111/j.1365-246X.1986.tb04553.x>
- Biryol, C. B., Wagner, L. S., Fischer, K. M., & Hawman, R. B. (2016). Relationship between observed upper mantle structures and recent tectonic activity across the Southeastern United States. *Journal of Geophysical Research: Solid Earth*, 121(5), 3393–3414. <https://doi.org/10.1002/2015JB012698>
- Boyce, A., Bastow, I. D., Golos, E. M., Rondenay, S., Burdick, S., & Van der Hilst, R. D. (2019). Variable modification of continental lithosphere during the proterozoic grenville orogeny: Evidence from teleseismic P-wave tomography. *Earth and Planetary Science Letters*, 525, 115763. <https://doi.org/10.1016/j.epsl.2019.115763>
- Brudner, A., Jiang, H., Chu, X., & Tang, M. (2022). Crustal thickness of the grenville orogen: A mesoproterozoic Tibet? *Geology*, 50(4), 402–406. <https://doi.org/10.1130/G49591.1>
- Chai, C., Ammon, C. J., Maceira, M., & Herrmann, R. (2022). Crust and upper mantle structure beneath the Eastern United States. *Geochemistry, Geophysics, Geosystems*, 23(3), e2021GC010233. <https://doi.org/10.1029/2021gc010233>
- Christensen, N. I., & Mooney, W. D. (1995). Seismic velocity structure and composition of the continental crust: A global view. *Journal of Geophysical Research*, 100(B6), 9761–9788. <https://doi.org/10.1029/95JB00259>

- Cook, F. A. (2002). Fine structure of the continental reflection Moho. *Bulletin of the Geological Society of America*, 114(1), 64–79. [https://doi.org/10.1130/0016-7606\(2002\)114<0064:fsotcr>2.0.co;2](https://doi.org/10.1130/0016-7606(2002)114<0064:fsotcr>2.0.co;2)
- Cook, F. A., & Vasudevan, K. (2006). Reprocessing and enhanced interpretation of the initial COCORP southern Appalachians traverse. *Tectonophysics*, 420(1–2), 161–174. <https://doi.org/10.1016/j.tecto.2006.01.022>
- Dickas, A. B., Mudrey, M. G., Ojakangas, R. W., & Shrike, D. L. (1992). A possible southeastern extension of the midcontinent rift system in Ohio. *Tectonics*, 11(6), 1406–1414. <https://doi.org/10.1029/91tc02903>
- Dilek, Y., & Furnes, H. (2014). Ophiolites and their origins. *Elements*, 10(2), 93–100. <https://doi.org/10.2113/gselements.10.2.93>
- Dumond, G., Williams, M. L., & Regan, S. P. (2018). The Athabasca granulite terrane and evidence for dynamic behavior of lower continental crust. *Annual Review of Earth and Planetary Sciences*, 46, 353–386. <https://doi.org/10.1146/annurev-earth-063016-020625>
- Fischer, K. M. (2002). Waning buoyancy in the crustal roots of old mountains. *Nature*, 417(6892), 933–936. <https://doi.org/10.1038/nature00855>
- Frederiksen, A. W., & Bostock, M. G. (2000). Modelling teleseismic waves in dipping anisotropic structures. *Geophysical Journal International*, 141(2), 401–412. <https://doi.org/10.1046/j.1365-246x.2000.00090.x>
- Funck, T., Louden, K. E., & Reid, I. D. (2000). Crustal structure of the Grenville Province in southeastern Labrador from refraction seismic data: Evidence for a high-velocity lower crustal wedge. *Canadian Journal of Earth Sciences*, 38(10), 1463–1478. <https://doi.org/10.1139/e01-026>
- Gao, H., & Li, C. (2021). Lithospheric formation and evolution of eastern North American continent. *Geophysical Research Letters*, 48(5). <https://doi.org/10.1029/2020GL091074>
- Gao, H., Yang, X., Long, M. D., & Aragon, J. C. (2020). Seismic evidence for crustal modification beneath the Hartford rift basin in the northeastern United States. *Geophysical Research Letters*, 47(17). <https://doi.org/10.1029/2020GL089316>
- Gorman, A. R., Clowes, R. M., Ellis, R. M., Henstock, T. J., Levander, A., Spence, G. D., et al. (2002). Deep probe: Imaging the roots of Western North America. *Canadian Journal of Earth Sciences*, 39(3), 375–398. <https://doi.org/10.1139/e01-064>
- Hacker, B. R., Kelemen, P. B., & Behn, M. D. (2015). Continental lower crust. *Annual Review of Earth and Planetary Sciences*, 43(1), 167–205. <https://doi.org/10.1146/annurev-earth-050212-124117>
- Hatcher, R. D., Jr. (2010). The Appalachian orogen: A brief summary. In R. P. Tollo, M. J. Bartholomew, J. P. Hibbard, & P. M. Karabinos (Eds.), *From Rodinia to Pangea: The lithotectonic record of the Appalachian region* (206). Geological Society of America. [https://doi.org/10.1130/2010.1206\(01\)](https://doi.org/10.1130/2010.1206(01))
- Heaman, L. M., & Kjarsgaard, B. A. (2000). Timing of eastern North American kimberlite magmatism: Continental extension of the great meteor hotspot track? *Earth and Planet Science Letters*, 178(3–4), 253–268. [https://doi.org/10.1016/S0012-821X\(00\)00079-0](https://doi.org/10.1016/S0012-821X(00)00079-0)
- Hibbard, J. P., Van Staal, C. R., Rankin, D. W., & Williams, H. (2006). *Lithotectonic MAP of the Appalachian orogen (MAP NO. 2096A, scale 1:5000000)*. Canada–United States of America: Geological Survey of Canada.
- Hinze, W. J., & Chandler, V. W. (2020). Reviewing the configuration and extent of the Midcontinent rift system. *Precambrian Research*, 342, 105688. <https://doi.org/10.1016/j.precamres.2020.105688>
- Huang, G., Guo, J., Jiao, S., & Palin, R. (2019). What drives the continental crust to be extremely hot so quickly? *Journal of Geophysical Research: Solid Earth*, 124(11), 11218–11231. <https://doi.org/10.1029/2019JB017840>
- Huang, Y., Chubakov, V., Mantovani, F., Rudnick, R. L., & McDonough, W. F. (2013). A reference Earth model for the heat-producing elements and associated geoneutrino flux. *Geochemistry, Geophysics, Geosystems*, 14(6), 2003–2029. <https://doi.org/10.1002/ggge.20129>
- Hughes, S., & Luetgert, J. H. (1992). Crustal structure of the southeastern Grenville province, northern New York state and eastern Ontario. *Journal of Geophysical Research*, 97(B12), 17455–17479. <https://doi.org/10.1029/92JB01793>
- Hynes, A., & Rivers, T. (2010). Protracted continental collision—Evidence from the Grenville orogen this article is one of a series of papers published in this special issue on the theme Lithoprobe—Parameters, processes, and the evolution of a continent. *Canadian Journal of Earth Sciences*, 47(5), 591–620. <https://doi.org/10.1139/E10-003>
- Indares, A., & Dunning, G. (1997). Coronitic metagabbro and eclogite from the Grenville province of Western Quebec: Interpretation of U-Pb geochronology and metamorphism. *Canadian Journal of Earth Sciences*, 34(7), 891–901. <https://doi.org/10.1139/e17-074>
- Jagoutz, O., & Kelemen, P. B. (2015). Role of arc processes in the formation of continental crust. *Annual Review of Earth and Planetary Sciences*, 43(1), 363–404. <https://doi.org/10.1146/annurev-earth-040809-152345>
- Jamieson, R. A., Beaumont, C., Warren, C. J., & Nguyen, M. H. (2010). The Grenville orogen explained? Applications and limitations of integrating numerical models with geological and geophysical data. *Canadian Journal of Earth Sciences*, 47(4), 517–539. <https://doi.org/10.1139/E09-070>
- Julia, J., Ammon, C. J., Herrmann, R. B., & Correig, A. M. (2000). Joint inversion of receiver function and surface wave dispersion observations. *Geophysical Journal International*, 143(1), 99–112. <https://doi.org/10.1046/j.1365-246x.2000.00217.x>
- Jull, M., & Kelemen, P. B. (2001). On the conditions for lower crustal convective instability. *Journal of Geophysical Research*, 106(B4), 6423–6446. <https://doi.org/10.1029/2000jb900357>
- Kay, R. W., & Kay, M. S. (1991). Creation and destruction of lower continental crust. *Geologische Rundschau*, 80(2), 259–278. <https://doi.org/10.1007/BF01829365>
- Kennett, B. L. N., Engdahl, E. R., & Buland, R. (1995). Constraints on seismic velocities in the Earth from travel times. *Geophysical Journal International*, 122(1), 108–124. <https://doi.org/10.1111/j.1365-246X.1995.tb03540.x>
- Kono, Y., Ishikawa, M., Harigane, Y., Michibayashi, K., & Arima, M. (2009). P- and S-wave velocities of the lowermost crustal rocks from the Kohistan arc: Implications for seismic Moho discontinuity attributed to abundant garnet. *Tectonophysics*, 467(1–4), 44–54. <https://doi.org/10.1016/j.tecto.2008.12.010>
- Leech, M. (2001). Arrested orogenic development: Eclogitization, delamination and tectonic collapse. *Earth and Planetary Science Letters*, 18(1–2), 149–159. [https://doi.org/10.1016/s0016-8002\(00\)00374-5](https://doi.org/10.1016/s0016-8002(00)00374-5)
- Li, C., Gao, H., & Williams, M. L. (2020). Seismic characteristics of the eastern North American crust with Ps converted waves: Terrane accretion and modification of continental crust. *Journal of Geophysical Research: Solid Earth*, 125(5). <https://doi.org/10.1029/2019JB018727>
- Ma, X., & Lowry, A. R. (2017). USArray imaging of continental crust in the conterminous United States. *Tectonics*, 36(12), 2882–2902. <https://doi.org/10.1002/2017TC004540>
- Marzen, R. E., Shillington, D. J., Lizarralde, D., Knapp, J. H., Heffner, D. M., Davis, J. K., & Harder, S. H. (2020). Limited and localized magmatism in the central Atlantic magmatic province. *Nature Communications*, 11(1), 3397. <https://doi.org/10.1038/s41467-020-17193-6>
- Mazza, S. E., Gazel, E., Johnson, E. A., Kunk, M. J., McAleer, R., Spotila, J. A., et al. (2014). Volcanoes of the passive margin: The youngest magmatic event in eastern North America. *Geology*, 42(6), 483–486. <https://doi.org/10.1130/G35407.1>
- McLelland, J. M., Selleck, B. W., & Bickford, M. E. (2010). Review of the proterozoic evolution of the Grenville province, its adirondack outlier, and the mesoproterozoic inliers of the Appalachians. In R. P. Tollo, M. J. Bartholomew, J. P. Hibbard, & P. M. Karabinos (Eds.), *From Rodinia to Pangea: The lithotectonic record of the Appalachian region* (206). Geological Society of America. [https://doi.org/10.1130/2010.1206\(02\)](https://doi.org/10.1130/2010.1206(02))

- McLelland, J. M., Selleck, B. W., & Bickford, M. E. (2013). Tectonic evolution of the Adirondack mountains and Grenville orogen inliers within the USA. *Geoscience Canada*, 40(4), 318–352. <https://doi.org/10.12789/geocanj.2013.40.022>
- Miller, D. J., & Christensen, N. I. (1994). Seismic signature and geochemistry of an island arc: A multidisciplinary study of the Kohistan accreted terrane, northern Pakistan. *Journal of Geophysical Research*, 99(B6), 11623–11642. <https://doi.org/10.1029/94jb00059>
- Mooney, W. D., & Kaban, M. K. (2010). The north American upper mantle: Density, composition, and evolution. *Journal of Geophysical Research*, 115(B12), B12424. <https://doi.org/10.1029/2010JB000866>
- Mount, V. S. (2014). Structural style of the Appalachian Plateau fold belt, north-central Pennsylvania. *Journal of Structural Geology*, 69, 284–303. <https://doi.org/10.1016/j.jsg.2014.04.005>
- Page, F. Z., Essene, E. J., & Mukasa, S. B. (2003). Prograde and retrograde history of eclogites from the eastern blue ridge, North Carolina, USA. *Journal of Metamorphic Geology*, 21(7), 685–698. <https://doi.org/10.1046/j.1525-1314.2003.00479.x>
- Petrescu, L., Bastow, I. D., Derbyshire, F. A., Gilligan, A., Bodin, T., Menke, W., & Levin, V. (2016). Three billion years of crustal evolution in eastern Canada: Constraints from receiver functions. *Journal of Geophysical Research: Solid Earth*, 121(2), 788–811. <https://doi.org/10.1002/2015JB012348>
- Ridley, V. A., & Richards, M. A. (2010). Deep crustal structure beneath large igneous provinces and the petrologic evolution of flood basalts. *Geochemistry, Geophysics, Geosystems*, 11(9), Q09006. <https://doi.org/10.1029/2009GC002935>
- Rivers, T. (1997). Lithotectonic elements of the Grenville province: Review and tectonic implications. *Precambrian Research*, 86(3–4), 117–154. [https://doi.org/10.1016/s0301-9268\(97\)00038-7](https://doi.org/10.1016/s0301-9268(97)00038-7)
- Rivers, T. (2008). Assembly and preservation of lower, mid, and upper orogenic crust in the Grenville province—Implications for the evolution of large hot long-duration orogens. *Precambrian Research*, 167(3–4), 237–259. <https://doi.org/10.1016/j.precamres.2008.08.005>
- Rondenay, S. (2009). Upper mantle imaging with array recordings of converted and scattered teleseismic waves. *Surveys in Geophysics*, 30(4–5), 377–405. <https://doi.org/10.1007/s10712-009-9071-5>
- Rudnick, R. L., & Fountain, D. M. (1995). Nature and composition of the continental crust: A lower crustal perspective. *Reviews of Geophysics*, 33(3), 267–309. <https://doi.org/10.1029/95RG01302>
- Rudnick, R. L., & Gao, S. (2013). Composition of the continental crust. *Geochemistry: Second edition*, 1–51. <https://doi.org/10.1016/B978-0-08-095975-7.00301-6.4>
- Saygin, E., & Kennett, B. L. N. (2012). Crustal structure of Australia from ambient seismic noise tomography. *Journal of Geophysical Research*, 117(1), 1304. <https://doi.org/10.1029/2011JB008403>
- Schmandt, B., Lin, F., & Karlstrom, K. E. (2015). Distinct crustal isostasy trends east and west of the Rocky Mountain Front. *Geophysical Research Letters*, 42(23), 10290–10298. <https://doi.org/10.1002/2015gl066593>
- Schulte-Pelkum, V., Mahan, K. H., Shen, W., & Stachnik, J. C. (2017). The distribution and composition of high-velocity lower crust across the continental US: Comparison of seismic and xenolith data and implications for lithospheric dynamics and history. *Tectonics*, 36(8), 1455–1496. <https://doi.org/10.1002/2017TC004480>
- Shalev, E., Park, J., & Lerner-Lam, A. (1991). Crustal velocity and Moho topography in central New Hampshire. *Journal of Geophysical Research*, 96(B10), 16415–16427. <https://doi.org/10.1029/91JB01591>
- Shen, W., & Ritzwoller, M. H. (2016). Crustal and uppermost mantle structure beneath the United States. *Journal of Geophysical Research: Solid Earth*, 121(6), 4306–4342. <https://doi.org/10.1002/2016JB012887>
- Stein, C. A., Stein, S., Elling, R., Keller, G. R., & Kley, J. (2018). Is the “Grenville front” in the central United States really the Midcontinent Rift? *Geological Society of America Today*, 28(5), 4–10. <https://doi.org/10.1130/GSATG357A.1>
- Stein, C. A., Stein, S., Merino, M., Keller, G. R., Flesch, L. M., & Jurdy, D. M. (2014). Was the mid-continent Rift part of a successful seafloor-spreading episode? *Geophysical Research Letters*, 41(5), 465–470. <https://doi.org/10.1002/2013GL059176>
- Sui, S., Shen, W., Mahan, K., & Schulte-Pelkum, V. (2022). Constraining the crustal composition of the continental U.S. using seismic observables. *GSA Bulletin*. <https://doi.org/10.1130/B36229.1>
- Wagner, L. S., Stewart, K., & Metcalf, K. (2012). Crustal-scale shortening structures beneath the blue ridge mountains, North Carolina, USA. *Lithosphere*, 4(3), 242–256. <https://doi.org/10.1130/L184.1>
- Whitmeyer, S., & Karlstrom, K. (2007). Tectonic model for the proterozoic growth of North America. *Geosphere*, 3(4), 220–259. <https://doi.org/10.1130/GES00055.1>
- Williams, M. L., Dumond, G., Mahan, K., Regan, S., & Holland, M. (2014). Garnet-forming reactions in felsic orthogneiss: Implications for densification and strengthening of the lower continental crust. *Earth and Planetary Science Letters*, 405, 207–219. <https://doi.org/10.1016/j.epsl.2014.08.030>
- Williams, M. L., Grover, T., Jercinovic, M. J., Regan, S. P., Pless, C. R., & Suarez, K. A. (2019). Constraining the timing and character of crustal melting in the Adirondack Mountains using multi-scale compositional mapping and in-situ monazite geochronology. *American Mineralogist*, 104(11), 1585–1602. <https://doi.org/10.2138/am-2019-6906>
- Williams, M. L., Scheltema, K. E., & Jercinovic, M. J. (2001). High-resolution compositional mapping of matrix phases: Implications for mass transfer during crenulation cleavage development in the Moretown formation, Western Massachusetts. *Journal of Structural Geology*, 23(6–7), 923–939. [https://doi.org/10.1016/S0191-8141\(00\)00164-4](https://doi.org/10.1016/S0191-8141(00)00164-4)
- Withjack, M. O., Schlische, R. W., & Olsen, P. E. (2012). Development of the passive margin of Eastern North America: Mesozoic rifting, igneous activity, and breakup. In *Regional geology and tectonics: Phanerozoic rift systems and sedimentary basins* (pp. 300–335). Elsevier Inc. <https://doi.org/10.1016/B978-0-444-56356-9.00012-2>
- Xia, Q., Zheng, Y., Lu, X., Hu, Z., & Xu, H. (2012). Formation of metamorphic and metamorphosed garnets in the low-T/UHP metagranite during continental collision in the Dabie orogen. *Lithos*, 136–139, 73–92. <https://doi.org/10.1016/j.lithos.2011.10.004>
- Zhang, H. L., Ravat, D., & Lowry, A. R. (2020). Crustal composition and moho variations of the central and eastern United States: Improving resolution and geologic interpretation of EarthScope USArray seismic images using gravity. *Journal of Geophysical Research: Solid Earth*, 125(3). <https://doi.org/10.1029/2019JB018537>